

INVESTIGATION OF CORE LOSSES IN SWITCHED RELUCTANCE MOTOR

*Pavol RAFAJDUS, *Valéria HRABOVCOVÁ **Peter HUDÁK

*Department of Power Electrical Systems, Faculty of Electrical Engineering University of Žilina, Univerzitná 1, 010 26 Žilina, Slovak Republic, tel.: 041/513 2158, E-mail: Pavol.Rafajdus@kete.utc.sk, Valeria.Hrabovcova@fel.utc.sk

**Power – One, s.r.o., Operations, Areal ZTS 924, 018 41 Dubnica nad Váhom, Slovak Republic, tel.: +421 42 44 07 316, E-mail: peter.hudak@power-one.com

SUMMARY

This paper deals with investigation of core losses in Switched Reluctance Motor (SRM), which is supplied by converter, if motor is loaded by rated torque and is running at various speeds. The core losses in the SRM consist mainly of hysteresis and eddy current losses. The winding losses are proportional to the square of the r.m.s current whereas the core losses are function of the excitation frequency and flux density, but the flux density depends on stator current waveforms. The different parts of the SRM core are subjected to the different frequency of flux reversals when the SRM is operating at constant speed and load. The detail analysis of flux linkage waveforms in individual parts of SRM magnetic system is performed. The current waveforms are not sinusoidal and depend on operating conditions. This paper deals with investigation of core losses in individual parts of SRM magnetic system by means of two analytical approaches for different rotor speed. The total core losses are calculated for the real 3-phase 12/8 SRM and verified by measurements.

Keywords: switched reluctance motor, iron losses, flux linkage, magnetic flux density

1. INTRODUCTION

Core losses prediction has an important role in design of electrical machine and in determination of its thermal rating. Efficiency optimization of the machine requires the sources of losses in the electrical machine and their relationships between the lamination material characteristic, machine dimensions, excitation conditions and losses. The determination of core losses of Switched Reluctance Motor (SRM) is complicated by the fact that the frequency of flux reversals is different in individual parts of the core [1], [2]. The complexity increases if the number of phases increases. The core losses ΔP_c in SRM are relatively low, even though the switching frequency is higher than in classical AC motors of the same speed and comparable pole number, and the flux waveforms in various parts of the magnetic circuit are not sinusoidal. The core losses are different for each part of SRM cross-section area, because the waveforms of flux linkage and flux density are different. In this paper the core losses are calculated by two analytical approaches. The flux linkage is calculated from real current and voltage waveforms in real 3-phase SRM, 12/8 (stator poles / rotor poles), 3.7kW, 3000rpm, 11.8 Nm [3], and verified by measurement of total core losses. The cross-section area of investigated SRM is shown in Fig. 1.

2. ANALYSIS OF FLUX LINKAGE WAVEFORM

Before calculation of SRM core losses it is very important to determine the flux linkage waveforms in each part of the core. The waveform of flux linkage in SRM depends on phase current waveform which depends on SRM speed and load. In the SRM only the stator winding is excited, the flux waveforms in the individual parts of core are

determined by the switching sequence in the stator phase winding. The normal switching sequence for 3-phase 12/8 SRM is to excite the phases successively, it means: A, B, C, A, B, C, etc (see Fig. 1).

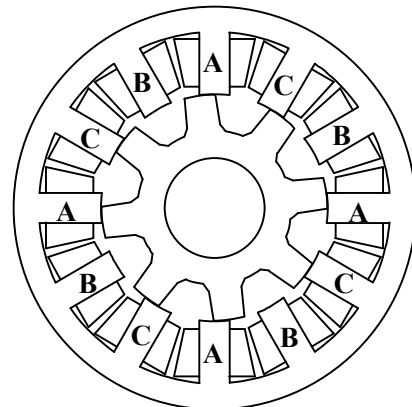


Fig. 1 The cross-section area of investigated SRM

In this case, each commutation step constitutes one working stroke and each cycle constitutes a switching period T_s . Since a phase winding is excited when a rotor pole tends to the alignment, the number of periods for stator phase per revolution is equal to the number of rotor poles. Then, the switching period per phase is given as

$$T_s = \frac{2\pi}{\omega_r N_R} = \frac{\lambda_r}{\omega_r} \quad (1)$$

where ω_r is angular speed of the rotor, N_R is number of rotor poles and λ_r is rotor pole pitch. In this case for rated speed 3000rpm is $T_s=0.0025$ s. The stroke period T_{st} depends on the number of phases. Each phase is excited once per cycle and it is given as:

$$T_{st} = \frac{T_s}{m} \quad (2)$$

which is for here investigated SRM at rated speed $T_{st}=0.00083s$.

The flux linkage frequency in the stator poles is determined from T_s as $f_s=1/T_s$, which is 400Hz and $f_{st}=1/T_{st}$, which is 1200Hz. These two frequencies provide the basis for the construction of flux linkage waveforms in all parts of the SRM core.

Flux linkage is different for each part of SRM as mentioned above, mainly in stator yoke, stator tooth, rotor yoke and rotor tooth. If the working point of rotor position is followed (Fig. 2), and the phases are switched successively, the idealised waveforms of flux linkage are obtained in individual parts of SRM cross-sections, see Fig. 2.

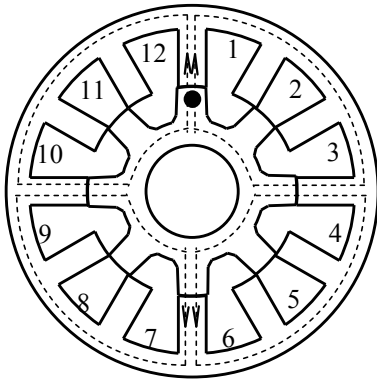


Fig. 2 The directions of SRM flux linkages as working point on the rotor rotates

2.1. Stator tooth flux linkage

In the Fig.3 there is only flux linkage waveform for phase A in stator tooth, which is reversed with period T_s , but it is only positive.

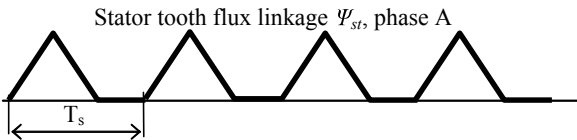


Fig. 3 The idealised stator tooth flux linkage waveform

2.2. Stator yoke flux linkage

The stator yoke of investigated SRM is possible to divide into 12 parts (see Fig. 2). The total flux linkage of the stator yoke parts is made as the sum of individual phase flux linkage waveforms. The construction of total flux linkage in parts 1,4,7,10 is shown in Fig. 4. From this Fig. it is clear, that the total flux is nearly constant, therefore the core losses

in these parts are negligible. However, in other parts of stator yoke (2,3,5,6,8,9,11,12) the flux linkage is reversed with period T_s , it is positive and negative and its waveform is shown in Fig. 5.

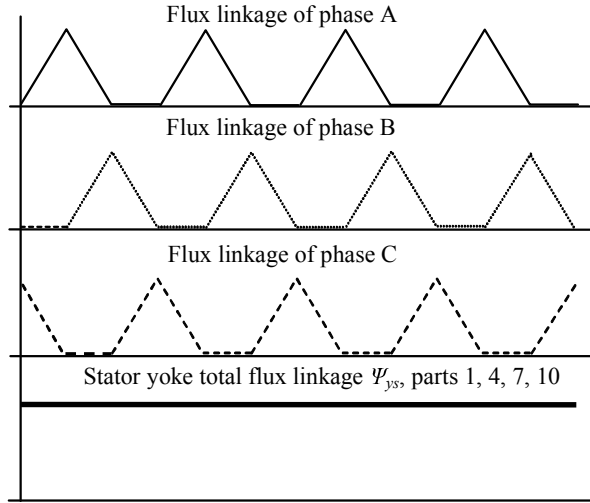


Fig. 4 The idealised stator yoke flux linkage waveforms in individual stator yoke parts 1,4,7,10

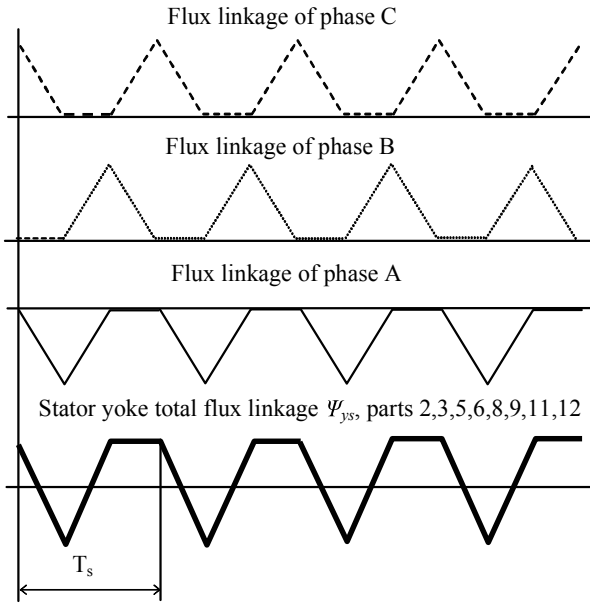


Fig. 5 The idealised stator yoke flux linkage waveforms in individual stator yoke parts 2,3,5,6,8,9,11,12

2.3. Rotor tooth flux linkage

The rotor tooth flux linkage waveform can be constructed and synthesized from the stator tooth waveform (see Fig. 3) by observing the phase relationship based on the following equation:

$$T_r = T_{st} \left(\frac{N_R}{2} \right) \quad (3)$$

Then the rotor tooth flux linkage waveform is shown in Fig. 6.

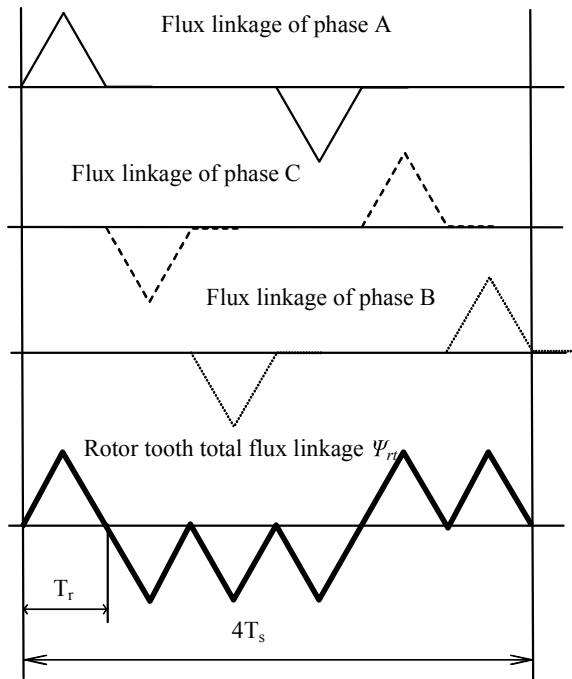


Fig. 6 The idealised rotor tooth flux linkage waveforms

2.4. Rotor yoke flux linkage

The total rotor yoke flux linkage, shown in Fig. 7 is made in similar way as the total stator yoke flux linkage in Fig. 5.

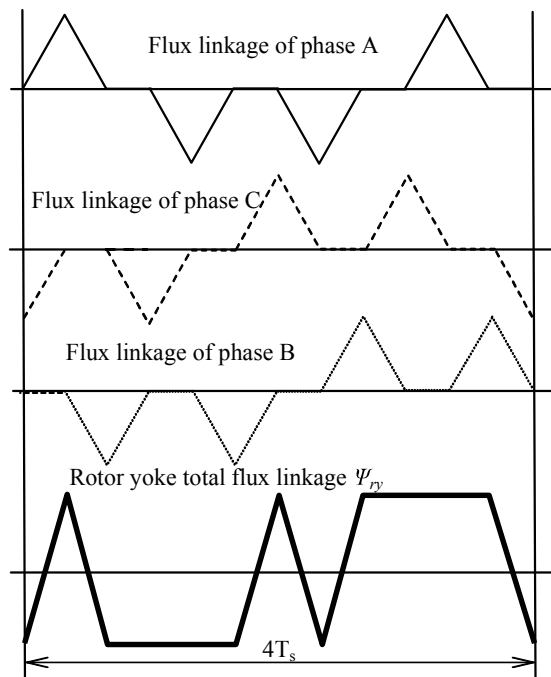


Fig. 7 The idealised rotor yoke flux linkage waveforms

From Fig. 6 and Fig. 7 it is evident, that the flux linkage in all rotor parts has frequency 4 times smaller than in stator parts. From this consideration it is possible to suppose that the rotor core losses are lower than in stator core.

The real flux linkage waveforms for different speed and rated torque have been calculated from measured waveforms of phase currents and voltages by means of equation:

$$\psi = \int (v - R_f i) dt \quad (4)$$

where R_f is the phase resistance, i is the phase current and v is phase voltage as functions of time for one period T_s .

The real flux linkage waveforms and calculated harmonics components of flux density for rated speed (3000rpm) and torque (11.8Nm) are shown in Fig. 8 for stator tooth, in Fig. 9 for stator yoke, where the flux linkage is negative and positive, in Fig. 10 for rotor tooth and in Fig. 11 for rotor yoke. In Fig. 8a, Fig. 9a, Fig. 10a and Fig. 11a the rotor position θ is on the x-axis in mechanical degrees, because the speed has been constant and it is possible to recalculate from time to mechanical degrees. In this real 12/8 SRM T_s equals 45° .

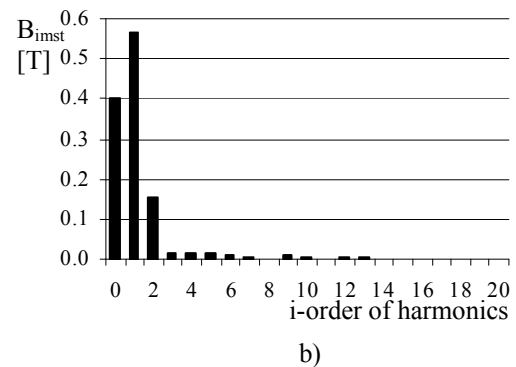
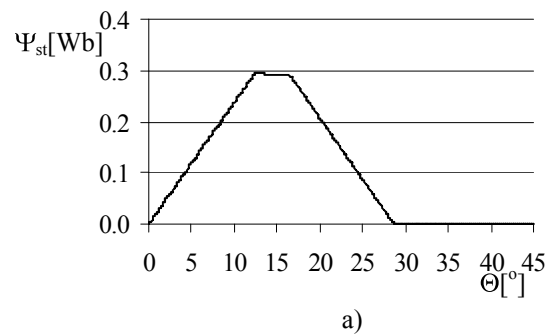
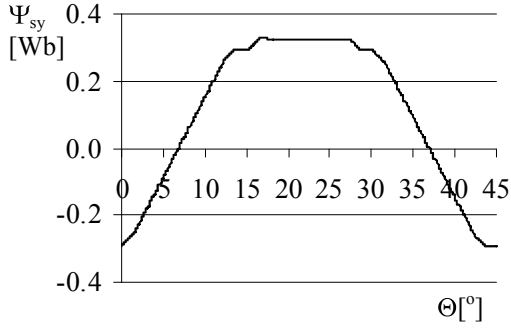
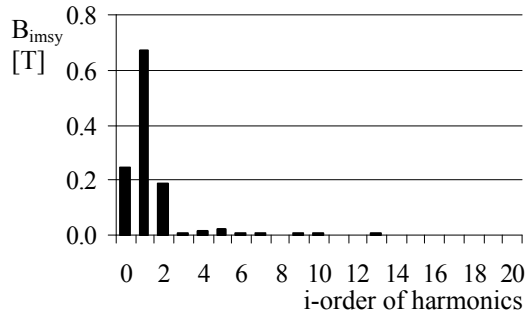


Fig. 8 a) The waveform of stator tooth flux linkage versus rotor position, b) magnitudes of flux density harmonic components

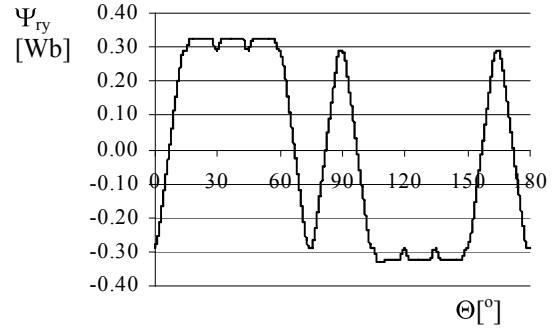


a)

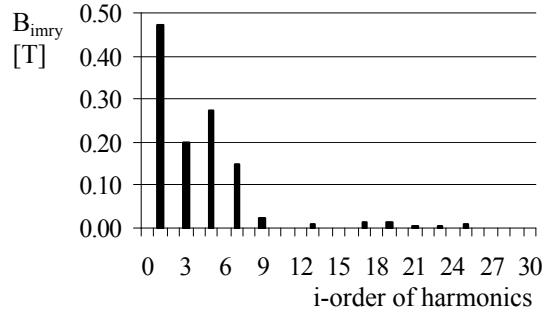


b)

Fig. 9 a) The waveform of stator yoke flux linkage versus rotor position, b) magnitudes of flux density harmonic components

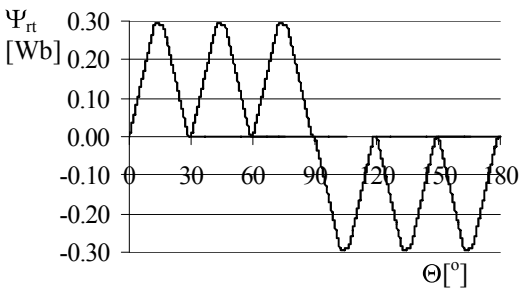


a)

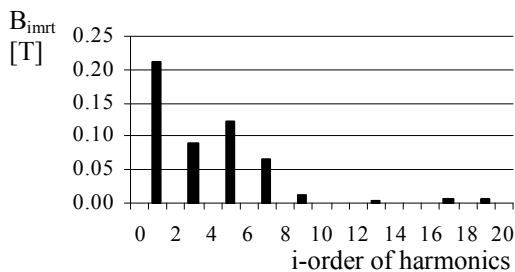


b)

Fig. 11 a) The waveform of rotor yoke flux linkage versus rotor position, b) magnitudes of flux density harmonic components



a)



b)

Fig. 10 a) The waveform of rotor tooth flux linkage versus rotor position, b) magnitudes of flux density harmonic components

3. CORE LOSSES CALCULATION

Core losses consist of both hysteresis loss and eddy current loss. To calculate hysteresis loss in the case of non-sinusoidal flux linkage waveform is a very difficult task. The most common method is to use modified Steinmetz equation for iron loss density, [4], [5], which is given as:

$$\Delta P_c = m(k_h f B_m^{a+bB_m} + k_e f^2 B_m^2) \quad (5)$$

where k_h and k_e are the coefficients of hysteresis and eddy-current loss given by manufacturer, a and b are constant of exponent, which depend on flux density magnitude and they are given as graph by manufacturer too, f is frequency, m is weight of correspondent part and B_m is flux density magnitude. This equation is valid for sinusoidal flux density.

As it can be seen from Fig. 8, Fig. 9, Fig. 10 and Fig. 11 the flux linkage waveforms are not sinusoidal, then some other approach has to be used.

3.1. Eddy current losses

For non sinusoidal waveform the harmonic analysis is needed for each flux linkage waveform to be able to calculate eddy current losses [6]. In accordance with the cross-section of correspondent SRM parts, the flux density magnitude calculation is needed. Then the eddy current losses are given as

$$\Delta P_{ce} = m \left(k_e \sum_{i=1} \left(\frac{f_i}{50} \right)^2 B_{im}^2 \right) \quad (6)$$

where ΔP_{ce} are eddy current losses, m is weight of correspondent part, k_e is factor of eddy current loss (it has been chosen 1.1 for dynamo sheets with thickness 0.5 mm and loss factor 2.6W/kg for frequency 50 Hz), f_i is frequency of harmonic components and B_{im} is magnitude of flux density, which is calculated from flux linkage and correspond cross-section area. From equation (6) all components of eddy current losses in stator teeth (st), stator yoke (sy), rotor teeth (rt) and rotor yoke (ry) are calculated step by step. They are summarized in Table I. for different speed and rated torque.

Speed [rpm]	500	1000	1500	2000	2500	3000
ΔP_{cest} [W]	2.95	10.77	19	27	35.4	43.7
ΔP_{cesy} [W]	17.7	37.4	74.1	93.1	122	150
ΔP_{cert} [W]	1.93	9.5	15.1	21.8	28.3	35.7
ΔP_{cery} [W]	1.75	6.9	17.1	17.5	22.8	20.7
ΔP_{ce} [W]	24.3	64.6	125	159	208	250

Table I. Eddy current losses

3.2. Hysteresis losses – the first approach

The calculation of hysteresis losses is more complicated than eddy current losses because equation (5) is defined for sinusoidal waveform and the harmonic analysis is not correct. If the coefficients and exponent of hysteresis losses from equation (5) are known, then is possible to use the flux density magnitude of non sinusoidal waveforms. In this case the hysteresis losses term of equation (5) is reduced by a factor of the “minor loop effect” in the hysteresis loop [4]. Because the coefficients, exponent and factor of minor loop effect of equation (5) for real here investigated SRM are unknown, the harmonic analysis has been used as estimated calculation of hysteresis losses. Some other authors use this method for calculation of hysteresis losses, [7]. Therefore it is also applied here but only as an informative value about hysteresis losses. Then the equation is given as:

$$\Delta P_{ch} = m \left(k_h \sum_{i=1} \left(\frac{f_i}{50} \right) B_{im}^2 \right) \quad (7)$$

where k_h is factor of hysteresis losses (it has been chosen 1.5 also for dynamo sheets mentioned above) and exponent has been taken 2.

In this paper this method is taken as the first approach with the subscript I. The total calculated hysteresis losses ΔP_{chl} are given as the sum of all core components. The hysteresis losses calculated in individual parts of SRM by the first approach I are

summarized in Table II. for different speed and rated torque.

Speed [rpm]	500	1000	1500	2000	2500	3000
ΔP_{chst} [W]	1.4	3.34	4.1	5.24	5.53	5.72
ΔP_{chsy} [W]	4.54	12.9	15.5	17.8	18.7	19.3
ΔP_{chrt} [W]	1.37	3.26	3.96	4.63	4.9	5.1
ΔP_{chry} [W]	1	2.61	4	3.63	3.93	3.8
ΔP_{chl} [W]	8.31	22.1	27.5	31.3	33.1	33.9

Table II. Hysteresis losses – the first approach

The total core losses are calculated as the sum of eddy current losses and hysteresis losses

$$\begin{aligned} \Delta P_{cl} &= \Delta P_{ch} + \Delta P_{ce} = \\ &= m \left(k_h \sum_{i=1} \left(\frac{f_i}{50} \right) B_{im}^2 + k_e \sum_{i=1} \left(\frac{f_i}{50} \right)^2 B_{im}^2 \right) \end{aligned} \quad (8)$$

The calculated values are shown in Table IV.

3.3. Hysteresis losses – the second approach

The second analytical approach is based on substitution of flux linkage non sinusoidal waveform by sinusoidal waveform with the same flux density magnitude. It is very simple method to calculate hysteresis core loss by means of classical equations. The flux density magnitudes are calculated from non sinusoidal flux linkage waveforms in stator and rotor parts (see Figures 8 - 11). For example, the substitution of waveform by sinusoidal waveform for rotor tooth is shown in Fig. 12. Then, the hysteresis core loss is calculated by following equation:

$$\Delta P_{ch} = m \left(k_h \frac{f}{50} B_m^2 \right) \quad (9)$$

and core losses according the second approach (subscript II) are given as follows:

$$\begin{aligned} \Delta P_{chl} &= \Delta P_{ch} + \Delta P_{ce} = \\ &= m \left(k_h \frac{f}{50} B_m^2 + k_e \sum_{i=1} \left(\frac{f_i}{50} \right)^2 B_{im}^2 \right) \end{aligned} \quad (10)$$

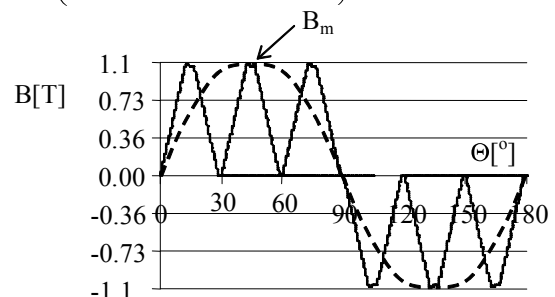


Fig. 12 Substitution of non sinusoidal flux density waveform in rotor tooth by sinusoidal waveform

The hysteresis losses calculated in individual parts of SRM by the second approach II are summarized in Table III. for different speed and rated torque.

The values of total iron losses ΔP_{cII} versus speed for rated torque from the second approach are also in Table IV.

Speed [rpm]	500	1000	1500	2000	2500	3000
ΔP_{chsr} [W]	2	6.55	8.32	10.1	9.15	8.4
ΔP_{chsy} [W]	8.3	24.8	39.1	48.5	43.3	42.8
ΔP_{chrl} [W]	3.4	5.1	7.12	10.2	7.7	7.2
ΔP_{chry} [W]	2	3.95	7.46	8.2	7.85	7.6
ΔP_{chII} [W]	15.7	40.4	62	77	68	66

Table III. Hysteresis losses – the second approach

Speed [rpm]	500	1000	1500	2000	2500	3000
ΔP_{cl} [W]	33	87	153	191	242	284
ΔP_{cII} [W]	40	105	187	236	276	316
ΔP_{cm} [W]	37	75	137	220	275	316

Table IV. The comparison of core losses

4. THE MEASUREMENT OF CORE LOSSES

The measurement of core losses have been made for total core losses only. The measurement of hysteresis and eddy current losses separately during operation is very difficult task.

The measured values of total core losses have been gained in such a way, that from the average electric power input P_{in} supplied to the motor, the winding, the additional and mechanical losses, and the output power P_m delivered on the shaft to a load have been subtracted. The mechanical losses have been measured by auxiliary calibrated DC motor and the additional losses due to their theoretical unpredictability, are appreciated by a certain percentage of the input power. In this measurement have been considered as 1% of the power input P_{in} .

The results of total core losses obtained by means of analytical approaches ΔP_{cl} , ΔP_{cII} are compared and verified by measurements ΔP_{cm} for rated torque and for different speed and they can be seen in the Table IV. It is seen that the second approach calculation gives the values in good coincidence with the measurement only at higher speed. For lower speeds it seems to be better to use the first approach.

5. CONCLUSION

The methods for core losses calculation in a real 12/8 3-phase SRM have been described. The detail analysis of flux linkage waveforms in individual parts of SRM magnetic system was performed. The calculation of core SRM losses was made by two analytical approaches, and calculated values are verified by measurement. Harmonic analysis has been used to determine the harmonic components of flux linkage and flux density in individual parts of the SRM core.

The core losses increase considerably as the level of speed increases. The first approach seems to be more suitable for lower speed (500-1500) rpm, because the percentage difference is no higher than 16%. In opposite, the second approach is more suitable for higher speed (>1500 rpm) because the percentage difference is no higher than 8%. The coincidence between calculations and measurements is very good. The used analytical methods are general and suitable also for others SRM, but the low and high speed range must be defined. The speed range and also frequency depends on control strategy and load and it can be different for various kind of SRM.

ACKNOWLEDGEMENT

This work was supported by Science and Technology Assistance Agency of Slovak Republic under the contract No. APVT-20-39602, by Grant No. 2003 SP 51/028 09 00/028 09 05 and by VEGA No. 1/2052/05

REFERENCES

- [1] Materu, P.; Krishnan, R.: Estimation of Switched Reluctance Motor Losses, 1988 IEEE, pp. 80-89
- [2] Metwally, H. M.; Faitz, J.; Finch, J. W.: Core Loss in Switched Reluctance Motor Structures: Experimental Results, ICEM 1988, pp. 31-34
- [3] Hrabovcová, V.; Rafajdus, P.; Ličko, M.; Janoušek, L.: Modelling of The Dynamic Operation of the Switched Reluctance Drive by Simulink, SPEEDAM'98, Sorrento, June, 3rd-5th 1998, Italy, pp. P1-61 – P1-66
- [4] Miller, T. J. E.: Switched Reluctance Motors and their Control. Magna Physics Publishing, Oxford 1993, ISBN 0-19-859387-2
- [5] Krishnan, R.: Switched Reluctance Motor Drives, Modeling, Simulation, Analysis, Design, and Applications, ISBN 0-8493-0838-0, CRC Press LLC 2001
- [6] Lamerraner, J.; Stafel M.: Eddy currents, ILIFE Books, London published in 1966

- [7] Saitz, J.: Magnetic Field Analysis of Induction Motors Combining Preisach Hysteresis Modeling and Finite Element Techniques, IEEE Trans. Magn., vol. 37, no. 5, pp. 3693–3697, September 2001
- [8] Miller, T.J.E.: Brushless permanent-magnet and reluctance motor drives, Oxford Science Publications, 1989, ISBN 0-19-859369-4
- [9] Ferková, Ž.; Zboray, L; Durovský, F.: Modelling and Control of Switched Reluctance Motor, Acta Electrotechnica et Informatica No. 2, Vol.2, 2002 str.14-18
- [10] Maga D., Hartanský R.: Numeric solving of electromechanic tasks, University of Trencin, Ludoprint Trencin, 2001, ISBN 80-88914-29-9
- [11] Bartos, V., Skala, B.: Sensitivity Analysis of an Asynchronous Machine under Transient Condition. In: 15th International Conference on Electrical Machines. Technologisch Instituut vzw: 380-380. Brugge - Belgium 2002. ISBN 90-76019-18-5

BIOGRAPHY

Pavol Rafajdus (MSc, PhD) graduated in electrical engineering from the University of Žilina, in Žilina in 1995 and 2002, respectively. At present he is a senior assistant at the Faculty of Electrical Engineering, University of Žilina. His research is focused on the reluctance electrical machines properties.

Valéria Hrabovcová (Prof, MSc, PhD), graduated in electrical engineering from the University of Žilina in Žilina, gained her PhD in electrical engineering from the Slovak University of Technology in Bratislava in 1985. She is a professor of electrical machines at the University of Žilina, Faculty of Electrical Engineering at undergraduate and postgraduate levels. Her professional and research interests include electronically commutated electrical machines.

Peter Hudák (MSc) received his MSc degree in electrical engineering from the University of Žilina (SK) in 2000. Formerly he was a PhD student at the University of Žilina. Now is with Power – One Company. His research activity is focused on electric machines, mainly on the reluctance synchronous motor.